New Method to Evaluate Negative-Ion Density Using Conventional Langmuir Probe

Engrhyt RATTANAWONGNARA[1)], Masaki OSAKABE[1,2)], Shingo MASAKI[1)], Katsuyoshi TSUMORI[1,2)], Haruhisa NAKANO[2,3)], Kenichi NAGAOKA[2,3)], Katsunori IKEDA[2)] and Yasuhiko TAKEIRI[2)]

[1)]*The Graduate University for Advanced Studies (SOKENDAI), 322-6 Oroshi, Toki, Gifu 509-5292, Japan*
[2)]*National Institute for Fusion Science, National Institutes of Natural Sciences, 322-6 Oroshi, Toki, Gifu 509-5292, Japan*
[3)]*Nagoya University, Furo-cho, Chikusa, Nagoya, Aichi 464-8601, Japan*

(Received 10 December 2022 / Accepted 14 February 2023)

A new experimental method using a Langmuir probe to measure negative-ion density is introduced in an area that cannot use lasers, such as the extraction hole. An electron reduction Langmuir probe model is established to distinguish negative ions from electron density. A comparison between density measured by the Langmuir probe with the electron reduction model and a photo-detachment Langmuir probe is performed to verify the use of the newly developed model.

Keywords: negative ion, negative-ion source, electronegative plasma, N-NBI, Langmuir probe

DOI: 10.1585/pfr.18.1401020

1. Introduction

A negative-ion based Neutral Beam Injector (N-NBI) is an essential heating device for ITER, DEMO, and future fusion reactors [1–3] to obtain high energy beams. The negative-ion source is the key component of N-NBI. In order to realize a high performance fusion reactor, highly efficient negative-ion beams are required. The efficiency of a negative-ion beam depends on the current ratio of negative ions to electrons (I_{H-}/I_e). If the ratio is small, the efficiency of the N-NBI becomes worse and moreover, the electron beam damages the electrodes of the ion source. It has been found that the formation of negative-ion rich plasma in beam extraction region of ion-source plasma is necessary to reduce the electron fraction of the extracted beam [4]. In the negative-ion source, hydrogen negative ions are produced on the caesiated surface of a plasma grid (PG). The transport process of negative ions from the surface to the beam extraction aperture is not clear, yet. Thus, we need to investigate the behavior of negative ions in the process.

The behavior of negative ions have usually been investigated by laser aided diagnostics using an electron photo-detachment process from negative ions. For example, the density of negative ions is obtained by a photo-detachment (PD) Langmuir probe [5] and/or a cavity ring down (CRD) diagnostic [6]. These diagnostics require an open laser path to the measurement region. On the other hand, it is quite difficult to forge a laser path inside the PG aperture where we need to investigate the behavior of negative ions. Therefore, a new technique to evaluate negative-ion density without a laser is required.

In this paper, we propose a method to evaluate negative-ion density using a conventional Langmuir probe. The negative-ion density obtained by the method is compared to that obtained with PD calibrated by CRD. In the following section, we describe the set-up of the experiment. In the third section, we explain the new method to evaluate the negative-ion density. The results are shown and discussed in the fourth section. The final section is the summary.

2. Experiment Set-Up

A schematic drawing of the Research and development Negative-Ion Source (RNIS) at the National Institute for Fusion Science (NIFS), i.e., NIFS-RNIS, is shown in Fig. 1 (a). The ion source consists of a driver region, where ion source plasma is generated, and an extraction region where the negative ions are extracted from the ion source plasma and is divided from the driver region by a filter magnet field. The source plasma is generated by a filament-arc discharge in a discharge chamber surrounded with multi-cusp magnets, as shown in the figure. The chamber has an inner volume of approximately 40 liters with a height (y-axis) of 700 mm, width (x-axis) of 350 mm, and depth (z-axis) of 230 mm. The caesium is seeded to enhance the surface production of negative hydrogen ions [7–9] and hydrogen gas is introduced at a pressure of 0.8 Pa. A typical negative-ion density of 2×10^{17} m^{-3} can be achieved with an arc discharge power of 50 kW in the NIFS-RNIS.

CRD measurement and photodetachment PD mea-

author's e-mail: engrhyt.rattanawongnara@nifs.ac.jp

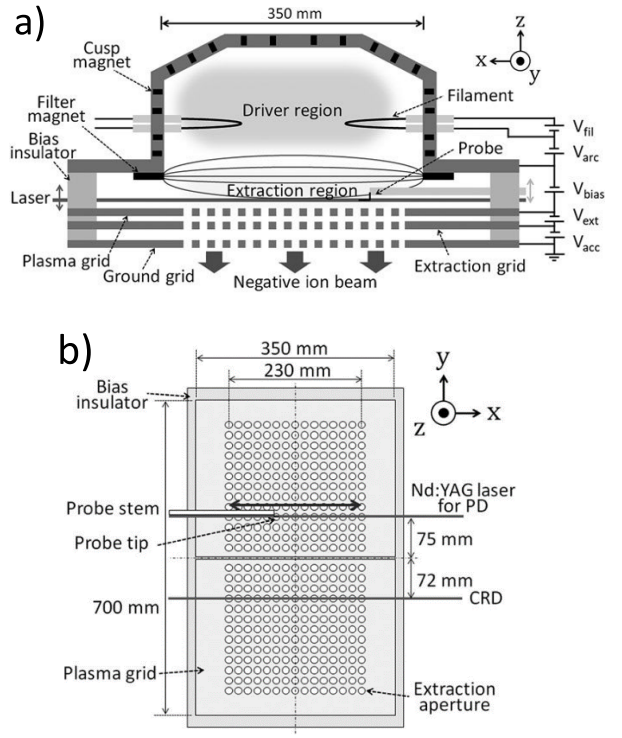

Fig. 1 (a) Horizontal cross section and (b) plasma grid view from backplate of NIFS-RNIS [10].

surement are setup to obtain negative-ion density in the RNIS. The CRD line of sight is located at −72 mm (y-direction) from the center of the PG, 15 mm (z-direction) from the PG surface, and the cavity path is aligned in parallel to the PG surface (x-direction), as shown in Fig. 1. The CRD is based on the attenuation of laser intensity by the photo-detachment process with negative ions. A short laser pulse is introduced from one side of a reflection cavity, which consists of a pair of mirrors with a reflectivity greater than 99.98%. Time dependence of laser intensity is measured by a photo-detector installed at the other end of the cavity. The decay time of laser intensity provides line integrated negative-ion density in the cavity [6].

PD Langmuir probe measurement (PDM) evaluates negative-ion density from the increment of electron saturation current of the Langmuir probe signal with a short laser pulse injection. When the laser is irradiated to plasmas containing negative ions, electrons are released from the negative ions inside the laser column as shown in Fig. 2. When negative-ion density is much smaller than electron density, the former can be evaluated from incremental electron saturation current, using an assumption of

$$n_-/n_e = \Delta I_e/I_e, \tag{1}$$

where n_-, n_e, I_e and ΔI_e are negative-ion density, electron density, electron saturation current and its increment, respectively [5]. When the negative-ion density becomes comparable to the electron density, this assumption may not be applicable to estimate the former, because I_e can-

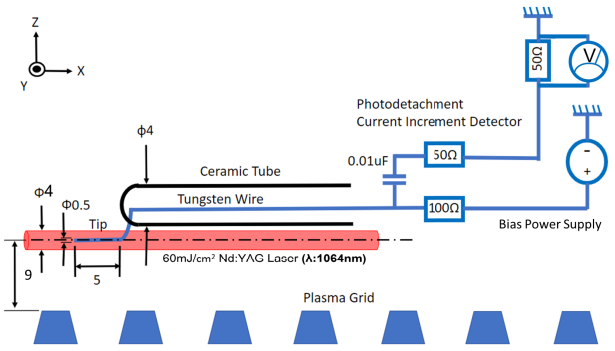

Fig. 2 Schematic drawing of PD along the Laser path [10].

not be evaluated from positively biased Langmuir probe currents, as the currents consist of both negative ions and electrons. In this case, it is necessary to calibrate the PDM using CRD measurement (CRDM). Since the CRDM is a line integrated measurement and the PDM is a local one, we need to perform an x-axis scan for the PDM to calibrate it with the CRDM, using Eqs. (2) and (3) [10].

$$k_{pd} \int \Delta I_e(x)dx = \left(\int_0^L n_-(x)dx \right)_{CRD}, \tag{2}$$

$$n_-(x) = k_{pd} \Delta I_e(x), \tag{3}$$

where L and k_{pd} are the path length of the CRDM and the calibration factor of the PDM. Note that the right-hand side term of Eq. (2) is directly measured by CRDM. In the NIFS-RNIS, the PDM is placed 75 mm apart from the ion source center in the y-direction, 9 mm in the z-direction and scans along the x-direction.

As shown in Fig. 2, the laser is fired in the x-direction from the opposite side of the PD probe diagnostic port. The diameter of the laser column is set at 2 mm, and the co-axis aligns with a cylindrical probe tip with a diameter of 0.5 mm [10]. A bias voltage of 40 V is applied to the probe tip to attract the electrons produced by the laser. That voltage is sufficient to measure the electron saturation current.

The PD Langmuir probe can also be used as a conventional Langmuir probe (LP) without the laser pulse. To use it as an LP, the bias voltage is scanned between −40 and 40 V for I-V measurement with a sweeping frequency of 20 Hz. Basically, current measured by the LP comes from two important mechanisms. First, the attraction and/or repulsion of charged particles by the electrostatic potential applied to the probe. Therefore, the LP is a charge selective measurement. Second, charge neutralization of ion and electron absorption at the probe tip produces probe current.

Typical I-V curves for caesiated and non-caesiated plasmas are shown in Fig. 3. In non-caesiated cases, the plasma is mainly composed of positive ions and electrons. Thus, the probe current due to negatively charged particles (I_-) is dominated by electrons. Because electron thermal

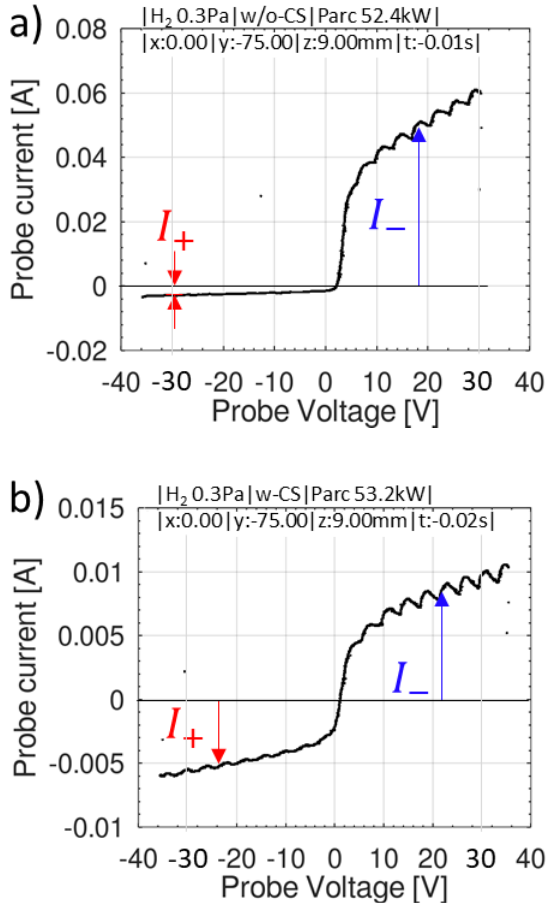

Fig. 3 I-V curve characteristic of (a) non-caesiated plasma and (b) caesiated plasma. Where I_+ mean positive charge and I_- means negative charge produced current *A ripple of curves comes from ripple of arc power supply through plasma responses.

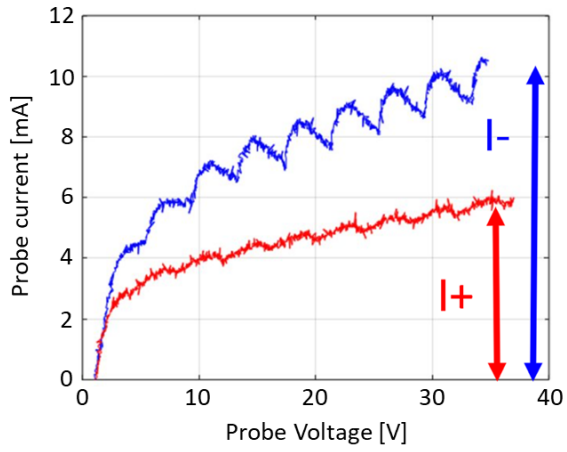

Fig. 4 Demonstration of unsymmetric of I_- and I_+ due to electron in electronegative plasma.

velocity is higher than that of positive ions, the I_- is always larger than the probe current, due to positively charged particles, (I_+) as shown in Fig. 3 (a). On the other hand, in non-caesiated case, the I-V curve becomes almost symmetric between I_- and I_+, as shown in Fig. 3 (b). This is because the density of negative ions becomes comparable to that of the positive ions. Plasma is called "electronegative plasma" in much literature [11–13]. Since small amounts of electrons can produce a large probe current, the density of negative ions in electronegative plasma cannot directly evaluate from the current. The absolute values of I_- and I_+ in Fig. 3 (b) with absolute probe-floating potential, shown in Fig. 4, emphasize that the I_- is larger than the I_+ because the former consists of electrons and negative ions.

3. Evaluation of Negative Ion Density by Conventional Langmuir Probe

In the evaluation of charged particle densities from the LP signal, the Orbital Motion Limit approximation (OML) is adopted [14]. The OML can provide density information from the LP signal without considering plasma temperature. The final form of the OML is written in Eqs. (4) - (6) which provide density information with the given mass and effective area value,

$$I_e = \frac{q_e A_e n_e}{2\pi}\sqrt{\frac{8q_e(V-V_p)}{m_e}}, \tag{4}$$

$$I_{i-} = \frac{q_{i-} A_i n_i}{2\pi}\sqrt{\frac{8q_{i-}(V-V_p)}{m_i}}, \tag{5}$$

$$I_{i+} = \frac{q_{i+} A_i n_i}{2\pi}\sqrt{\frac{8q_{i+}(V-V_p)}{m_i}}, \tag{6}$$

where I_e, I_{i-}, I_{i+} stand for electrons, negative ions, and positive ion currents of the probe signals, respectively. The A_e and A_i stand for the electron and ion effective area of the probe, V is probe applied potential, V_p refers to wall potential plus sheath potential, q_e, q_{i-}, q_{i+} are the charge of a particle, and m_e, m_i are electron mass and ion mass respectively. We assume that the probe absorbtion area of the ions is the same between the positive and negative ion and use the probe geometrical area (A_{geo}), as shown in Eq. (7) for the ions as it has a large Larmor radius compared to the electrons. The EDM field may not affect the probe ion absorption area.

$$A_i \approx A_{geo} = 2\pi rl + \pi r^2, \tag{7}$$

where $r = 0.25$ mm is the probe radius and $l = 10$ mm is the probe tip length.

The OML approximation is derived with an assumption that the sheath radius is 5 - 10 times larger than the probe radius when probe bias reaches the current saturation region. The effect of sheath variation by a shielding mechanism is thought to be negligible and the temperature of electrons or negative ions is cancelled out in the approximation.

As seen in Eqs. (4) to (6), the OML describes the saturation region current of the I-V curve as a square root

function. The slope of $I^2 - V$ can be evaluated for density information when it is linear enough [15]. For this reason, we consider the potential (floating point as a reference) between −30 to −15 volts for the positive charge saturation region and 15 to 30 volts for the negative charge saturation region. The evaluation of a slope in electron/electropositive plasma can be derived from Eqs. (4) and (5) which can be derived into,

$$\frac{dI_e^2}{dV} = -\left(\frac{q_e A_e n_e}{2\pi}\right)^2 \frac{8e}{m_e}, \tag{8}$$

$$\frac{dI_{i+}^2}{dV} = \left(\frac{q_{i+} A_i n_i}{2\pi}\right)^2 \frac{8e}{m_i}. \tag{9}$$

The unit of Eqs. (8) and (9) is a current square which can be reduced to Eqs. (10) and (11).

$$\sqrt{\frac{dI_e^2}{dV}} = \frac{qA_e n_e}{2\pi}\sqrt{\frac{8e}{\pi m_e}}, \tag{10}$$

$$\sqrt{\frac{dI_+^2}{dV}} = \frac{qA_i n_i}{2\pi}\sqrt{\frac{8e}{\pi m_i}}. \tag{11}$$

The density evaluation of the OML theory can be described in short form as Eqs. (12) and (13), which is applied to current shown Fig. 5 (a) for non-caesiated plasma density evaluation.

$$n_e = \frac{2\pi}{qA_e}\sqrt{\frac{\pi m_e}{8q}}\sqrt{\frac{dI_e^2}{dV}}, \tag{12}$$

$$n_{i+} = \frac{2\pi}{qA_i}\sqrt{\frac{\pi m_i}{8q}}\sqrt{\frac{dI_+^2}{dV}}. \tag{13}$$

According to charge neutrality the properties of plasma and the non-caesiated version, maintains a balance between a positive charge and mostly electrons. The OML theory here is focused on electron and positive-ion density. After evaluating the I^2-V slope in Fig. 5 (a), "beta", a current coefficient, is introduced to distinguish the current difference of electrons and positive ions which become Eq. (14). The beta obtained from the definition in Eq. (13) is plotted versus the arc power shown in Fig. 6. The empirical beta value will be used in the next step. However, the plot indicates that at high arc power, the beta value reaches factor $\sqrt{m_i/m_e} \sim 42$ and at low arc power the value decreases with a logarithmic function. The behavior of beta leads to a prediction that probe area factor A_e/A_i is the cause of beta decreasing at low arc power when electrons are under the influence of a magnetic field [16] which is applied at the source.

$$\beta \equiv \frac{A_e}{A_i}\sqrt{\frac{m_i}{m_e}}. \tag{14}$$

With the OML theory and the empirical "beta" coefficient, the new "electron reduction Langmuir probe model" is constructed for separate electron components from negative ion current. As a first step, we consider current from electrons and negative ions, mixed in the probe current,

$$I_- = I_{i-} + I_e. \tag{15}$$

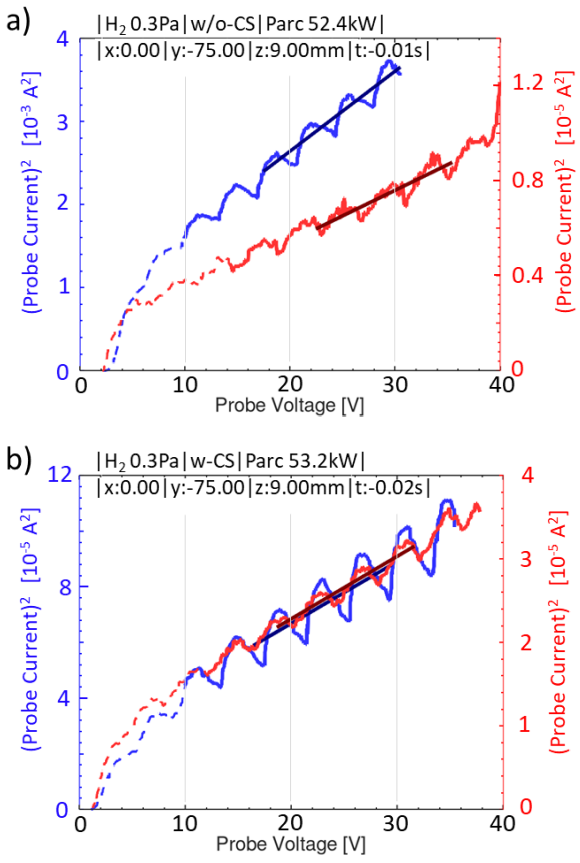

Fig. 5 I^2-V curve used for OML evaluation, curve in red is positive saturation current, curve in blue is negative saturation current, (a) non-caesiated cause (b) caesiated cause. Dashed line indicates retard region, continuous line saturation region. Black line is a fitting for density evaluation.

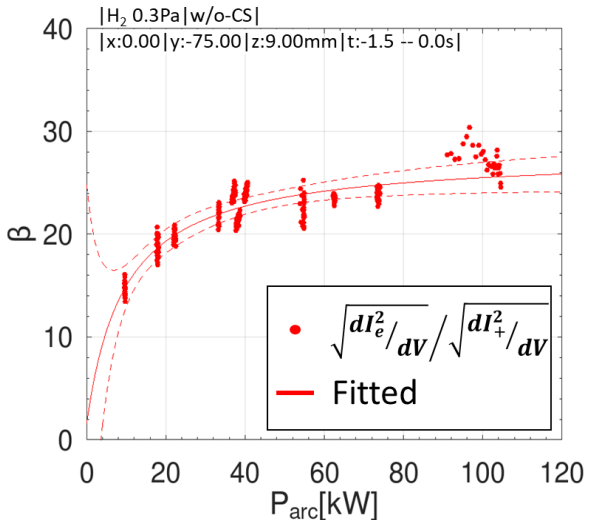

Fig. 6 Empirical plot of beta value versus arc power from non-caesiated plasma.

Second, as we consider the OML theory, the square root function in the saturation region of the plasma is assumed for all species. With properties of the OML as an *I-V* function of each species is a square root function. Therefore density information of electron and negative ion is independent, as shown in Eqs. (16) to (18),

$$I_- = \frac{qA_i n_{i-}}{2\pi}\sqrt{\frac{8q(V-V_p)}{\pi m_i}} + \frac{qA_e n_e}{2\pi}\sqrt{\frac{8q(V-V_p)}{\pi m_e}}, \tag{16}$$

$$I_-{}^2 = \left(\frac{qA_i n_{i-}}{2\pi}\sqrt{\frac{8q}{\pi m_i}} + \frac{qA_e n_e}{2\pi}\sqrt{\frac{8q}{\pi m_e}}\right)^2 (V-V_p), \tag{17}$$

$$\frac{dI_-^2}{dV} = \left(\frac{qA_i n_{i-}}{2\pi}\sqrt{\frac{8q}{\pi m_i}} + \frac{qA_e n_e}{2\pi}\sqrt{\frac{8q}{\pi m_e}}\right)^2. \tag{18}$$

Here the OML allows a determination of electrons and negative ions as an independent current source, shown in Eqs. (19) and (20),

$$\sqrt{\frac{dI_-^2}{dV}} = \frac{qA_i n_{i-}}{2\pi}\sqrt{\frac{8q}{\pi m_i}} + \frac{qA_e n_e}{2\pi}\sqrt{\frac{8q}{\pi m_e}}, \tag{19}$$

$$\sqrt{\frac{dI_+^2}{dV}} = \frac{qA_i n_{i+}}{2\pi}\sqrt{\frac{8q}{\pi m_i}}. \tag{20}$$

Third, utilize charge neutrality to balance between triple particles,

$$n_{i+} = n_{i-} + n_e. \tag{21}$$

Fourth, apply the "beta" coefficient from non-caesiated plasma to eliminate electron term,

$$\beta = \frac{A_e}{A_i}\sqrt{\frac{m_i}{m_e}}. \tag{22}$$

With the contribution of Eqs. (19) to (22), negative-ion density is described in Eq. (23),

$$n_- = \frac{I^-_{OML} - \beta I^+_{OML}}{\frac{qA_i}{2\pi}\sqrt{\frac{8q}{\pi m_i}}(1-\beta)} = \frac{\sqrt{\frac{dI_-^2}{dV}} - \beta\sqrt{\frac{dI_+^2}{dV}}}{\frac{qA_i}{2\pi}\sqrt{\frac{8q}{\pi m_i}}(1-\beta)}. \tag{23}$$

With Eq. (23), we can evaluate the negative-ion concentration of plasma using the slope fitted in Fig. 5 (b). The arc power dependence plot shown in Fig. 7 is a result of the LP with the OML electron reduction method and PDM. The density value from both diagnostics varies between 0 - 5×10^{17} m^{-3}.

The negative-ion densities evaluated by the LP with the electron reduction method are compared to those evaluated by PDM and are shown in Fig. 8. As can be seen in the figure, these two densities are linearly correlated.

The linear dependence of the LP measurement on PDM shows that the negative-ion density evaluation by the LP with the electron reduction method well expresses the densities of negative ions, although it needs a correction by a factor of 0.648, using the PDM as a reference. The appearance of correction factor comes from two important sources. First, as we assumed that $A_i \sim A_{geo}$; however the EDM field may strong enough to affect the ion absorbtion area of the probe for this analysis, and the discrepancy between actual A_i to the given A_{geo}, contributes to the correction factor. Second, the validity of the OML theory is limited due to the change of plasma sheath. The saturation region in the actual *I-V* curve may not follow the square root function as described in the OML [17–19]. However, the linearity between the two measurements in this research is high enough to use this simple correction factor. This enables us to measure the densities of negative ions where laser aided diagnostics cannot be applied.

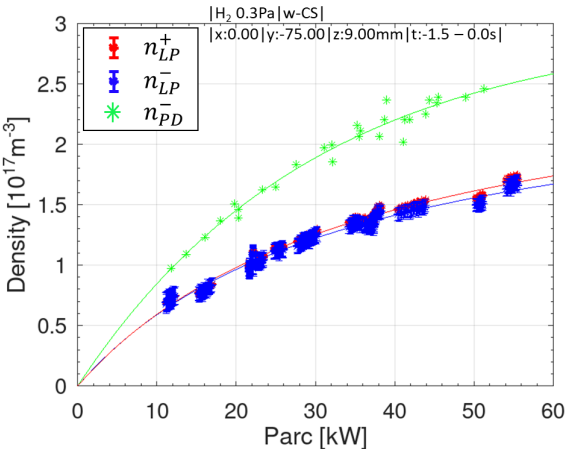

Fig. 7 Arc power dependence of positive and negative-ion densities evaluated by LP with electron reduction method and negative-ion densities evaluated by PDM.

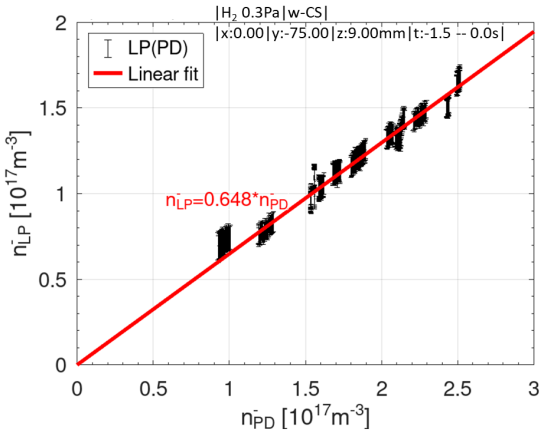

Fig. 8 Comparison of negative-ion densities evaluated by PDM and by LP measurement.

4. Conclusion

We have demonstrated that negative-ion density measurement with LPM and the electron reduction method can

be applied by comparing the result with density measured by PDM. The electron reduction method is constructed from the famous OML theory which allows negative-ion evaluation in the presence of electrons in plasma. For this reason, negative-ion density measurement can be done without the laser aided method in obstructed places, with simple LP, for instance, in the extraction hole and reaching the wall area of the negative-ion source.

[1] R.S. Hemsworth *et al*., New J. Phys. **19**, 025005 (2017).
[2] F. Bonomo *et al*., Fusion Eng. Des. **159**, 111760 (2020).
[3] C. Hopf *et al*., Nucl. Fusion **61**, 106032 (2021).
[4] K. Tsumori and M. Wada, New J. Phys. **19**, 045002 (2017).
[5] H. Nakano *et al*., AIP Conf. Proc. **1390**, 359 (2011).
[6] M. Bacal *et al*., Plasma Sources Sci. Technol. **2**, 190 (1993).
[7] K. Nagaoka *et al*., AIP Conf. Proc. **1390**, 374 (2011).
[8] K. Tsumori, H. Nakano, M. Kisaki *et al*., Rev. Sci. Instrum. **83**, 02B116 (2012).
[9] H. Nakano, K. Tsumori, M. Kisaki *et al*., AIP Conf. Proc. **1515**, 237 (2013).
[10] S. Masaki *et al*., Rev. Sci. Instrum. **91**, 013512 (2020).
[11] J. Bredin *et al*., Phys. Plasmas **21**, 123502 (2014).
[12] K. Miyamoto *et al*., Plasma Sources Sci. Technol. **31**, 105012 (2022).
[13] R.N. Franklin *et al*., Plasma Sources Sci. Technol. **11**, A31 (2002).
[14] H.M. Mott-Smith and I. Langmuir, Phys. Rev. **28**, 727 (1926).
[15] H.A. Hamad *et al*., Int. J. Thin. Fil. Tec. **8**, 83 (2019).
[16] M. Usoltceva *et al*., Phys. Plasmas **25**, 063518 (2018).
[17] S.H. Lam, Phys. Fluids **8**, 73 (1965).
[18] J.G. Laframboise, Ph.D. thesis, University of Toronto (1966).
[19] Ch. Steinbrüchel, J. Vac. Sci. Technol. **A8** (3), 1663 (1990).